2021 3rd International Conference on Control Systems, Mathematical Modeling, Automation and Energy Efficiency (SUMMA) | 978-1-6654-3981-7/21/$31.00 ©2021 IEEE | DOI: 10.1109/SUMMA53307.2021.9632193

Meshfree Approximate Solution of the Cauchy–Navier Equations of Elastodynamics

Svilen S. Valtchev
CEMAT, IST, University of Lisbon
ESTG, Polytechnic of Leiria, Portugal
ssv@math.ist.utl.pt

Nuno F. M. Martins
Department of Mathematics, FCT
Universidade Nova de Lisboa, Portugal
nfm@fct.unl.pt

***Abstract*—In this study we propose a meshfree scheme for the numerical solution of boundary value problems (BVP) for the nonhomogeneous Cauchy-Navier equations of elastodynamics. The method uses the classical approach where first a particular solution for the partial differential equation (PDE) is calculated and then the corresponding homogeneous BVP is solved for the homogeneous part of the total solution. In particular, we approximate each component of the source term of the nonho-mogeneous PDE by superposition of plane wave functions with different frequencies and directions of propagation. Using these expansions, a particular solution for the PDE is derived in the form of a linear combination of elastic P- and S-waves, at no extra computational cost. In the second step of the scheme, we solve the corresponding homogeneous BVP using the classical method of fundamental solutions (MFS), with shape functions given by the Kupradze tensor. The accuracy and the convergence of the proposed technique is illustrated for a Dirichlet BVP, posed in a 2D multiply connected domain, bounded by polygonal and parametric curves.**

Keywords—meshfree method, plane wave functions, method of fundamental solutions, Cauchy-Navier equations of elastodynamics, nonhomogeneous PDE.

I. Introduction

In this work we address the problem of elastic wave propagation in a homogeneous isotropic material subjected to a body force. In particular, we consider the interior wave scattering problem where our goal is to recover the scattered wave $\mathbf{u}^{sc}$ generated by the interaction between a known incident wave $\mathbf{u}^{inc}$ and an obstacle with known material properties. For rigid obstacles, the total wave $\mathbf{u}^{tot} = \mathbf{u}^{inc} + \mathbf{u}^{sc}$ vanishes on the boundary of the domain and mathematically the problem may be formulated as a Dirichlet boundary value problem (BVP) with boundary condition of the form $\mathbf{u}^{sc} = -\mathbf{u}^{inc}$.

Let $\Omega \subset \mathbb{R}^2$ be a bounded domain with a class C^1 boundary $\Gamma = \partial\Omega$. In time harmonic settings, for a given body force with intensity $\mathbf{f}$, the displacement field $\mathbf{u} = \mathbf{u}^{sc}$ satisfies. the Dirichlet BVP for the nonhomogeneous Cauchy-Navier equations of elastodynamics

$$\begin{cases}(\Delta * + \rho\omega^2)\mathbf{u} = \mathbf{f} & \text{in } \Omega,\\ \boldsymbol{u} = \mathbf{g} & \text{on } \Gamma\end{cases} \quad (1)$$

where $\Delta*$ is the linear elastic (Lame) operator defined by

$$\Delta * = \mu\Delta + (\lambda + \mu)\nabla\nabla, \quad (2)$$

$\omega > 0$ is a constant frequency, $\rho > 0$ is the constant density of the material and $\lambda > 0$ and $\mu > 0$ are material-dependent constants called Lame parameters. Note that problem (1) is well posed if $-\rho\omega^2$ is not an eigenvalue for the Lame operator $\Delta*$ in Ω, e.g. [1]. Under this assumption, for $\mathbf{f} \in [L^2(\Omega)]^2$ and $\mathbf{g} \in [H^{1/2}(\Gamma)]^2$, the BVP has a unique solution $\mathbf{u} \in [H^1(\Omega)]^2$.

One possible approach for calculating an approximate solution of problem (1) is to use an appropriate variant of the method of fundamental solutions (MFS). According to its original formulation, see [2], [3], the MFS is a meshfree method for the numerical solution of homogeneous partial differential equations (PDE) where the unknown solution of the BVP is approximated by a linear combination of fundamental solutions of the differential operator with singularities (source points) located in the exterior of the domain of interest. Since such linear combinations belong to the solution space of the homogeneous PDE, the MFS requires only an accurate fitting of the boundary conditions of the BVP. This is usually done by discrete collocation or using a least squares approach.

The MFS has attracted significant attention from the scientific community due to its straightforward implementation, low computational cost and high accuracy in smooth settings, see [4] for an overview of the MFS. As a result, many variants of the MFS have been developed and successfully applied to direct and inverse, interior and exterior and linear and nonlinear problems in acoustics, electromagnetism, elasticity, fluid mechanics, heat conduction, options pricing, shape optimization, etc., see [5]–[8] and the references therein.

In [9], we have proposed a numerical scheme related to the MFS, where the solution of problem (1) is approximated by a linear combination of fundamental solutions (Kupradze tensors) of the Cauchy-Navier operator $\Delta*+\rho\omega^2$ with different test frequencies and source points. This method requires the solution (in the least squares sense) of a large and fully populated ill-conditioned linear system, where the PDE and the boundary conditions are collocated simultaneously, using sets of domain and boundary collocation knots. Although the basis functions in this method are related to the differential operator, which significantly simplifies its formulation and im-plementation, this method is still computationally demanding for BVP in complex geometries and higher dimensions.

The first author gratefully acknowledges the financial support from the Portuguese FCT - Fundacao para a Ciencia e a Tecnologia, through the projects UIDB/04621/2020 and UIDP/04621/2020 of CEMAT/IST-ID, Center for Computational and Stochastic Mathematics, Instituto Superior Tecnico, University of Lisbon, Portugal.

978-1-6654-3981-7/21/$31.00 ©2021 European Union

In order to alleviate the high computational cost of the method presented in [9], a classical two-step approach may be considered for the solution of problem (1). In this case, we represent the solution u in the form

$$\mathbf{u} = \mathbf{u}^{\mathrm{P}} + \mathbf{u}^{\mathrm{H}}, \quad (3)$$

where $\mathbf{u}^{\mathrm{P}}$ is a particular solution of the PDE

$$(\Delta * + \rho\omega^2)\mathbf{u}^{\mathrm{P}} = \mathbf{f}, \quad \text{in } \Omega \quad (4)$$

and $\mathbf{u}^{\mathrm{H}}$ satisfies the corresponding homogeneous BVP

$$\begin{cases} (\Delta * + \rho\omega^2)\mathbf{u}^{\mathrm{H}} = 0 & \text{in } \Omega, \\ \mathbf{u}^{H} = \mathbf{g} - \mathbf{u}^{\mathrm{P}} & \text{on } \Gamma \end{cases} \quad (5)$$

In the framework of meshfree methods, a particular solution of equation (4) is usually calculated in terms of a linear combination of radial basis functions (RBF), e. g. thin plate splines, multiquadrics, etc., using the dual reciprocity method (DRM), see [10] – [13]. Problem (5) is then solved using a meshfree method, e. g. the classical MFS. However, deriving a particular solution using the DRM may be a mathematically elaborate process, e.g. [14], especially in the case of a vector PDE like (4).

In section II, we propose an alternative method for the calculation of the particular solution of problem (4). We begin by approximating each component of the body force $\mathbf{f} = (f_1, f_2)$ by a linear combination of plane wave functions with different test frequencies and directions of propagation. The approximation properties of these shape functions are well documented in the literature, e.g. [15], [16]. Next, by rescaling the coefficients of the plane wave expansions, we derive an approximation for the particular solution $\mathbf{u}^{\mathrm{P}}$ in the form of a linear combination of pressure (P) and shear (S) elastic waves. This is done at no extra computational cost. In section III, we present the formulation of the classical MFS for the homogeneous problem (5). Here, for the fundamental solution of the Cauchy-Navier operator we use the symmetric Kupradze tensor, see [17]. In section IV, we test the performance of the proposed scheme for a BVP posed in a multiply connected domain, bounded by polygonal and parametric curves.

In the following discussion we will consider the two-dimensional case of problem (1) and, in order to simplify the notation, we will assume that the elastic media $\mathbf{\Omega}$ has a unitary density $\rho = 1$. The generalization of the proposed method to tree-dimensional problems is straightforward, taking into account the expected increase in the computational cost due to the solution of larger linear systems. We also note that the fundamental solution of the Cauchy-Navier operator in the three-dimensional case involves exponential functions which can be evaluated much faster than the Bessel functions required in the two-dimensional case.

II. A Particular Solution for the PDE

For a set of N_0 distinct unitary directions

$$D = \{\mathbf{d}_1, \mathbf{d}_2, \dots, \mathbf{d}_{\mathrm{N}_0}\} \subset \mathrm{S}^1$$

and a set o P_0 distinct positive test frequencies

$$K = \{\kappa_1, \kappa_2, \dots, \kappa_{\mathrm{P}_0}\} \subset \mathrm{R}+,$$

we approximate each component of function $\mathbf{f} = (f_1, f_2)$ separately, by superposition of (scalar) plane wave functions

$$f_\ell(\mathrm{x}) \approx \tilde{f}_\ell(\mathrm{x}) = \sum_{p=0}^{P_0} \sum_{n=1}^{N_0} \alpha_{p,n}^{l} W_{K_p}(x, \mathbf{d}_n), \;\; l = 1,2, \quad (6)$$

where $W_{\mathrm{K}}(x, \mathbf{d}) = \exp(i\kappa\, x \cdot \mathbf{d})$ is a plane wave with frequency κ and direction of propagation $\mathbf{d}$, $i = \sqrt{-1}$ and $\alpha^{\ell}_{p,n} \in \mathrm{C}$ are unknown coefficients.

The coefficients $\alpha^{\ell}_{p,n}$ are calculated by collocating function f_ℓ using a set of M_0 distinct collocation points

$$X_0 = \{x_1, x_2, \dots, x_{M_0}\} \subset \Sigma,$$

selected in an arbitrary, e.g. rectangular, domain $\Sigma \supset \overline{\Omega}$. This process leads to the solution of two linear systems of the form

$$[\mathrm{W}\kappa_1\,(\mathrm{X}_0, \mathrm{D}) \dots \;\; \mathrm{W}_{\kappa_{\mathrm{P}_0}}(\mathrm{X}_0, \mathrm{D})][\mathrm{a}_\ell] = [f_\ell(\mathrm{X}_0)], \quad (7)$$

where $\mathrm{a}_\ell = \{\alpha_{1,1}^{l}, 1, \dots, \alpha_{P_0,N_0}\}$ and W_κ is a basic matrix block defined by

$$[\mathrm{W}\kappa_1\,(X_0, D) = \begin{bmatrix} W_\kappa(x_1, \mathbf{d}_1) & \cdots & W_\kappa(x_1, \mathbf{d}_{N_0}) \\ \vdots & \ddots & \vdots \\ W_\kappa(x_{M_0}, \mathbf{d}_1) & \cdots & W_\kappa(x_{M_0}, \mathbf{d}_{N_0}) \end{bmatrix} \quad (8)$$

System (7) is ill-conditioned and it may be solved in the least squares sense, with $\mathrm{M}_0 > \mathrm{P}_0 \times \mathrm{N}_0$, e. g. using truncated singular value decomposition (TSVD) regularization [18]. Also, from a theoretical point of view, approximation (6) is justified in terms of the following density result for plane wave functions, see [19]

$$L^2(\Sigma) = \overline{\mathrm{span}\{W_\kappa(x, \mathbf{d})|_{\mathrm{x}\in\Sigma} : \kappa \in \mathrm{R}+, \mathbf{d} \in \mathrm{S}^1\}}. \quad (9)$$

After solving systems (7), the vector valued body force f can be approximated by the linear combination

$$\mathbf{f}(\mathrm{x}) \approx \tilde{\mathbf{f}}(\mathrm{x}) = \sum_{p,n} a_{p,n} W_{K_p}(x, \mathbf{d}_n), \quad (10)$$

where $a_{p,n} = (a_{p,n}^1, a_{p,n}^2) \in \mathbb{C}^2$ are vector coefficients.

Next, for a given unitary direction $\mathbf{d}_{\mathrm{n}}$ and a test frequency κ_{p}, we define the two types of elastic plane waves

$$\begin{aligned} \phi_{p,n}(x) &= \mathbf{d}_n\, W_{\kappa_p}(x, \mathbf{d}_n)(\mathrm{P-wave}) \\ \psi_{p,n}(x) &= \mathbf{d}_n^{\perp}\, W_{\kappa_p}(x, \mathbf{d}_n)(S-\mathrm{wave}) \end{aligned} \quad (11)$$

where $\mathbf{d}_n^{\perp}$ is a direction that is orthogonal to $\mathbf{d}_n$. Using these definitions and the decomposition

$$\mathbf{a}_{p,n} W_{K_p}(x, \mathrm{d}_n) = (a_{p,n} \cdot \mathrm{d}_n)\, \phi_{p,n}(x) + (a_{p,n} \cdot \mathrm{d}_n^{\perp})\, \psi_{p,n}(x) \quad (12)$$

we represent $\tilde{\mathbf{f}}$ in the form of a linear combination of elastic P- and S-waves

$$\tilde{\mathbf{f}}(\mathrm{x}) = \sum_{p,n} (a_{p,n} \cdot \mathbf{d}_n)\phi_{p,n}(x) + (a_{p,n} \cdot \mathbf{d}_n^{\perp})\psi_{p,n}(x), \quad (13)$$

Finally, noting that the two types of elastic waves satisfy

$$(\Delta* + \omega^2)\phi_{p,n}(x) = (\omega^2 - \kappa_p^2(\lambda + 2\mu))\phi_{p,n}(x)$$
$$(\Delta* + \omega^2)\psi_{p,n}(x) = (\omega^2 - \kappa_p^2\mu)\psi_{p,n}(x) \quad (14)$$

we can write the approximate solution $\tilde{\boldsymbol{u}}^P$ of equation (4) as a linear combination of elastic P- and S-waves as follows

$$\tilde{\boldsymbol{u}}^P(x) = \sum_{p,n} \frac{a_{p,n} \cdot d_n}{\omega^2 - \kappa_p^2(\lambda + 2\mu)} \phi_{p,n}(x) + \frac{a_{p,n} \cdot d_n^{\perp}}{\omega^2 - \kappa_p^2\mu} \psi_{p,n}(x), \quad (13)$$

Note that, in order to calculate $\tilde{\boldsymbol{u}}^P$, only the solution of the two linear systems (7) is required. Also, to ensure that $\tilde{\boldsymbol{u}}^P$ is well defined, we assume that the test frequencies $\kappa_p \in K$ are such that $\omega^2 - \kappa_p^2(\lambda + 2\mu) \neq 0$ and $\omega^2 - \kappa_p^2\mu \neq 0$.

III. MFS Solution of the Homogeneous Problem

The fundamental solution for the two-dimensional scalar Helmholtz operator $\Delta + \kappa^2$ is given by

$$\Phi_\kappa(x) = \frac{i}{4} H_0^{(1)}(\kappa \parallel x \parallel), \quad (16)$$

where $\parallel \cdot \parallel$ is the Euclidian norm and $H_0^{(1)} = J_0 + iY_0$ is the Hankel function of the first kind and order zero, defined in terms of the Bessel functions of the first and second kind and order zero, J_0 and Y_0, respectively. Note that $\Phi_\kappa(x)$ is a radially symmetric function and, due to the logarithmic singularity of Y_0, its real part is singular at $x = 0$.

In the elastic case, for a given frequency $\omega > 0$, two types of waves (P and S) are propagated, with wavenumbers, κ_P and κ_S, depending on the properties of the elastic media and defined by

$$\kappa_p^2 = \frac{\omega^2}{\lambda + 2\mu} \ (\text{P} - \text{wave}), \ \kappa_S^2 = \frac{\omega^2}{\mu} \ (S - \text{wave}) \quad (17)$$

The fundamental solution for the elastodynamics operator $\Delta*$ + ω^2 is defined in terms of the fundamental solutions of the scalar Helmholtz equation with wavenumbers κ_P and κ_S and it is given by the symmetric Kupradze tensor, see [17]

$$G_\omega = \frac{1}{\omega^2}\left(\kappa_S^2 \Phi_{\kappa_S} I + D(\Phi_{\kappa_S} - \Phi_{\kappa_P})\right) \quad (18)$$

where I is the identity matrix and $D = [\partial_{ij}^2]$ is the second order derivative operator. Note that, in $\mathbb{R}^2 \setminus \{0\}$, G_ω is an analytic function and satisfies the homogeneous Cauchy-Navier PDE. A simplified form of (18), using the properties of the Hankel functions and their derivatives, can be found in [9].

An analytic particular solution for the homogeneous Cauchy-Navier PDE in $\boldsymbol{\Omega}$ may be defined by shifting the singularity of the Kupradze tensor to an exterior point $y \notin \boldsymbol{\Omega}$, called a source point. In the classical MFS formulation, we use a set of N1 such points

$$Y = \{y_1, y_2, \ldots, y_{N_1}\} \subset R^2 \setminus \bar{\Omega}$$

to define an approximation for the solution u^H of problem (5) in the form of a linear combination of fundamental solutions

$$\boldsymbol{u}^H(x) \approx \tilde{\boldsymbol{u}}^H(x) = \sum_{j=1}^{N_1} G_\omega(x - y_j)\beta_j \quad (19)$$

with unknown coefficients $\beta_j \in C^2$. Note that finding the optimal location of the source points for the MFS is a long standing open problems for this method, see [20] – [22]. In this study, we will consider that $Y \subset \hat{\Gamma}$, where Γ is the boundary of a larger domain, enclosing $\bar{\Omega}$.

According its definition, $\tilde{\boldsymbol{u}}^H$ is a solution for the PDE in problem (5) and it remains to calculate the unknown coefficients β_j by collocating the boundary conditions. This is done using a set of M_1 boundary collocation points

$$X = \{x_1, x_2, \ldots, x_{M_1}\} \subset \Gamma$$

and the process leads to the solution of the block linear system

$$\begin{bmatrix} G_\omega(x_1 - y_1) & \cdots & G_\omega(x_1 - y_{N_1}) \\ \vdots & \ddots & \vdots \\ G_\omega(x_{M_1} - y_1) & \cdots & G_\omega(x_{M_1} - y_{N_1}) \end{bmatrix} [\mathbf{b}]=[\mathbf{h}] \quad (8)$$

where $\mathbf{b} = \{\beta_1,..., \beta_{N_1}\}$ and $\mathbf{h} = \mathbf{g}(X_1) - \tilde{\boldsymbol{u}}^P(X_1)$.

In the case $M_1 = N_1$ system (20) can be solved using Gaussian elimination. However, this system is ill-conditioned and better numerical results can be achieved by solving it in the least squares sense, with $M_1 > N_1$, and using Tikhonov or TSVD regularization

IV. Numerical Results

In this section we apply the numerical scheme proposed in sections II–III to problem (1) posed in the multiply connected domain $\boldsymbol{\Omega} = P \setminus \{C_1 \cup C_2\}$, where P is the polygon defined by the vertices $\{(-1, -1), (1, -1), (1, 0), (0, 1), (-1,1)\}$ and C_1, C_2 are two circles with radius 0.25 and centers (0, −0.5) and (−0.5, 0.5), respectively, see Fig. 1.

Two examples will be considered for the numerical tests. In the first one, in order to validate the method, we pre-select the exact solution $\mathbf{u} = (u_1, u_2)$ of the BVP and then calculate (analytically) the Dirichlet boundary condition $\mathbf{g}$ and the body force $\mathbf{f}$. In this case, the quality of the approximate solution $\tilde{\mathbf{u}}$ = $(\tilde{u}_1, \tilde{u}_2)$ will be evaluated by measuring the error

$$\varepsilon_\Omega := \max_{\ell=1.2} \|u_\ell - \tilde{u}_\ell\|_{L^2(\bar{\Omega})} \quad (21)$$

In the second example, we consider non-matching boundary and domain functions $\mathbf{g}$ and $\mathbf{f}$ and the exact solution of the BVP is not available. Here, we infer about the quality of $\tilde{\mathbf{u}}$ by

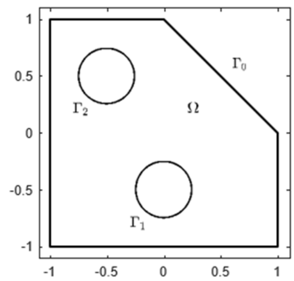

Fig. 1. Domain for Examples 1 and 2.

measuring two types of approximation error. First, we analyse the domain collocation error of the forcing term approximation

$$\varepsilon_\Omega := \max_{\ell=1.2} \left\| f_\ell - \tilde{f}_\ell \right\|_{L^2(\Omega)}$$

This error is directly related to the approximation error of the particular solution $\tilde{\mathbf{u}}^P$, which is calculated by rescaling the coefficients of $\tilde{\mathbf{f}}$, see (15). The second type of error we analyse here is the boundary error of $\tilde{\mathbf{u}}^H$

$$\varepsilon_\Gamma := \max_{\ell=1.2} \left\| g_\ell - \tilde{u}_\ell^P - \tilde{u}_\ell^H \right\|_{L^2(\Gamma)}$$

where $\mathbf{g} = (g_1, g_2)$, $\tilde{\mathbf{u}}^P = (\tilde{u}_1^P, \tilde{u}_2^P)$ and $\tilde{\mathbf{u}}^H = (\tilde{u}_1^H, \tilde{u}_2^H)$. Note that, by the well posedness of problem (5) and since the classical MFS is a Trefftz type method, the approximation error of $\tilde{u}^H$ in Ω is bounded in terms of ε_Γ, e.g. [1]. Finally, using the triangle inequality, the error of $\tilde{\mathbf{u}}$ in Ω may be bounded as follows

$$\max_{\ell=1.2} \| u_\ell - \tilde{u}_\ell \|_{L^2(\Omega)} \leq K_1 \varepsilon_\Omega + K_2 \varepsilon_\Gamma$$

where $K_1 > 0$ and $K_2 > 0$ are appropriate constants.

Remark 1: The errors ε, ε_Γ and ε_Ω will be estimated using the discrete l2 norm which is equivalent to the root-mean-square (RMS) error

$$\| v - \tilde{v} \|_2 = \left(\frac{1}{\#Z} \sum_{z \in Z} | v(z) - \tilde{v}(z) |^2 \right)^{1/2}$$

where Z is a large set of domain or boundary error test points.

A. *Example 1 – known exact solution*

We consider problem (1) with frequency $\omega = 3.5$, Lame parameters $\lambda = 1$ and $\mu = 2$ and exact solution

$$\boldsymbol{u}(x) = \{ x_1^2 \sin(\pi x_2), x_2^2 \cos(\pi x_1) \}$$

Accordingly, the Dirichlet boundary condition on Γ is defined by restriction on Γ, $\mathbf{g} = \mathbf{u}|_\Gamma$, and the forcing term is calculated analytically as $f = (\Delta * + \omega^2)\mathbf{u}$.

For the plane wave approximation of the body force f we considered $N_0 = 25$ unitary directions, uniformly distributed on the unit sphere S^1 and $P_0 = 10$ integer test frequencies from the set $K = \{1, 2, ..., 10\}$. We collocated each com-ponent of $\mathbf{f} = (f_1, f_2)$ using an uniform grid of $M_0 = 400$ points in the square domain $\Sigma = [-1.2, 1.2]^2 \supset \bar{\Omega}$.

The resulting two linear systems were solved using the mldivide Matlab function, with a residual RMS error of order 10^{-7}. For the collocation error in Ω we measured $\varepsilon_\Omega = 1.25 \times 10^{-7}$, using a set of 70450 error test knots. From this approximation of the body force, a particular solution $\tilde{u}^P$ was obtained by recalculating the coefficients of the plane wave expansions, see (15).

To solve problem (5) for the homogeneous part of the solution, we considered a set of $M_1 = 1042$ boundary collocation knots, uniformly distributed on $\Gamma = \Gamma_0 \cup \Gamma_1 \cup \Gamma_2$ with an approximate density of 100 points per unit length of arc. For the source points, we took the artificial boundary $\Gamma = \Gamma_0 \cup \Gamma_1 \cup \Gamma_2$, see [22], where $\hat{\Gamma}_\ell = 0.9 \times \Gamma_\ell$, $\ell = 1,2$ and Γ_0 lies at a constant distance of $\delta = 0.05$ from Γ_0. Approximately 50 source points per unit length of arc were considered here, which corresponds to a total of $N_1 = 531$ points. An example of the knot distribution for the MFS solution of problem (5) is shown in Fig. 2.

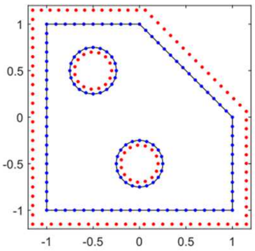

Fig. 2. Knot configuration for the MFS.

The above knot configuration corresponds to a linear system with dimensions 2084×1062 which was solved with a residual RMS error of order 10^{-6}. Using 4166 error test points, we measured $\varepsilon_\Gamma = 7.98 \times 10^{-6}$ for the boundary error of $\tilde{u}^H$.

For this example, since its exact solution is available, it is also possible to measure the RMS error of the total approximate solution $\tilde{\mathbf{u}} = \tilde{\mathbf{u}}^P + \tilde{\mathbf{u}}^H$ in $\bar{\Omega}$. In particular, for 70450 error test knots, we obtained $\varepsilon = 9.46 \times 10^{-7}$. The corresponding maximum absolute error was of order 10^{-4} and no significant error accumulation was observed near the corners or the edges of the domain.

It should be noted that an accurate approximation for the body force f, and consequently for the particular solution u^P, is essential for the performance of the numerical scheme since problem (5) involves $\tilde{\mathbf{u}}^P$ in the boundary condition.

As it is common for meshfree methods, higher accuracy may be achieved by increasing the number of test frequencies, unitary directions and collocation and source points. For example, by taking $N_0 = 70$, $P_0 = 40$ and $M_0 = 3600$ we calculated an approximation for the body force with an RMS error of $\varepsilon_\Omega = 5.87 \times 10{-}11$, which represents a decrease of 4 orders of magnitude in comparison with the previous results. A better approximation for the particular solution allowedus to obtain a more precise homogeneous solution and consequently a more accurate approximation for the total solution of the BVP. More precisely, for the solution of problem (5) we took $M_1 = 1573$ boundary collocation points and $N_1 = 10628$ source points, with the same distributions as before. The corresponding linear system was solved with a residual RMS error of order 10^{-13} and we measured a boundary error of $\varepsilon = 6.39 \times 10^{-12}$. For the total approximate solution $\tilde{u}$ the RMS error was $\varepsilon = 9.34 \times 10^{-14}$, which corresponds to an improvement of 7 orders of magnitude in comparison with the previous results. The corresponding maximum absolute error was of order 10^{-11}.

Note that the precision of the above numerical results is close to the maximum machine precision and therefore no significant further improvement is possible. These results also validate the implementation and the applicability of the proposed numerical scheme.

B. *Example 2 – unknown exact solution*

For this example we consider problem (1) with frequency $\omega = 2$, Lame parameters $\lambda = 1$ and $\mu = 3$, forcing term

$$\mathbf{f}(x) = \{\exp(x_1 + x_2), \sin(2\pi x_1)\exp(2x_2)\},\ x \in \Omega$$

and Dirichlet boundary condition

$$\mathbf{g}(x) = \begin{cases} \frac{1}{5}\{\sin(4\pi x_1 x_2), \cos(4\pi x_1 x_2)\} & \text{on } \Gamma_0 \\ 1 & \text{on } \Gamma_1 \cup \Gamma_2 \end{cases}$$

Note that functions **g** and **f** are unrelated and therefore the exact solution of the BVP is not known here.

For the plane wave approximation of function **f**, we took $P_0 = 40$ non-integer test frequencies from the set $K = \{i - 0.5 : i = 1,2,...,40\}$, $N_0 = 70$ unitary directions and $M_0 = 3600$ collocation points. The corresponding RMS error in the domain was $\varepsilon_\Omega = 1.81 \times 10{-}11$ and the absolute error of each component of **f** in **Ω** is shown in Fig. 3.

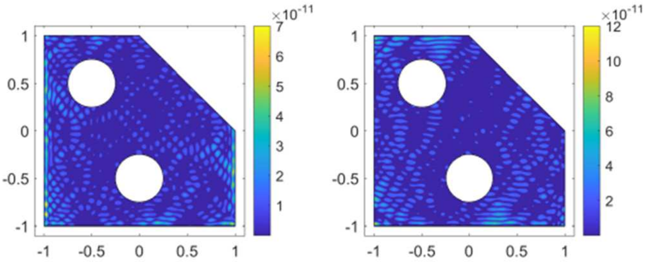

Fig. 3. Absolute error of $\tilde{f}_1$ and $\tilde{f}_2$ in Ω

For the solution of problem (5) we took $N_1 = 1571$ source points and $M_1 = 2083$ collocation points, with the same distributions as before. We measured $\varepsilon_\Gamma = 4.68 \times 10{-}6$ for the boundary RMS error. As expected, the maxima of the absolute error occur near the corners of the domain, see Fig. 4. This fact is due to the singularities of the solution, induced

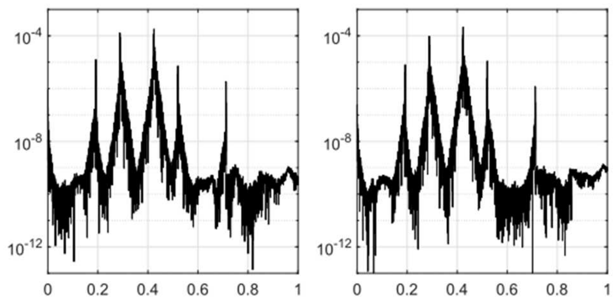

Fig. 4. Absolute error of $\tilde{u}^H$ (left) and $\tilde{u}^H$ (right) on Γ. Semi-log scale. Normalized arc length of Γ.

by the geometric singularities of the boundary, which cannot be accurately approximated by the analytic fundamental solutions. A possible approach to tackle this issue can involve a subtraction of singularity technique or an enrichment of the MFS approximation basis by a set of singular particular solutions of the PDE, see [23].

In Fig. 5 we present the plot of the real part of the approximate solution ũ in $\overline{\Omega}$. Note that ũ is a complex valued

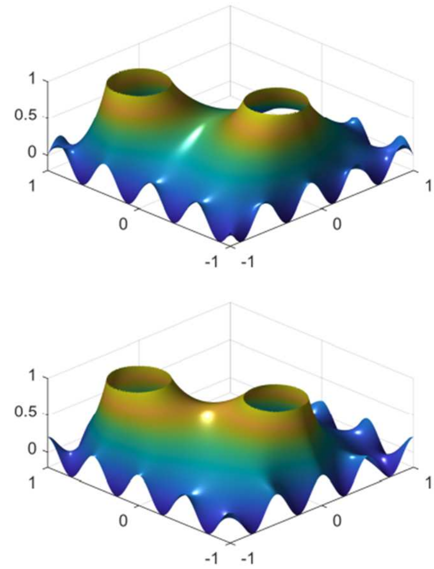

Fig. 5. Real part of the first and second component of u in Ω.

function and therefore, since the problem data **f** and **g** are both real functions, the magnitude of its imaginary part can give us an idea about the quality of the approximation. In fact, in the last simulation the imaginary part of u is neglectable, with an order of magnitude of 10^{-9}

We also tested the numerical scheme for higher values of the frequency ω in problem (1). In particular, we took ω = 5,10,20 and kept the remaining parameters of the BVP and the method as in the previous simulation. Since the source term in the PDE was kept unchanged, the error of the particular solution remained the same and we measured only the boundary error of the MFS solution of problem (5). The corresponding numerical results are presented in Table I.

TABLE I
RMS ERROR OF $\tilde{\mathbf{u}}^H$ ON Γ FOR $\omega = 5, 10, 20$.

ω	ε_Γ
5	5.84×10^{-6}
10	6.50×10^{-5}
20	1.26×10^{-4}

The results from Table I indicate that, for a fixed knot configuration, the accuracy of the MFS solution decreases when the value of the frequency is increased. This is the expected behavior since the frequency of the problem is directly related to the complexity of the solution.

V. CONCLUSIONS

In this work, a meshfree technique was presented for the numerical solution of BVP for the nonhomogeneous Cauchy-Navier equations of elastodynmics. An approximate solution of the problem was calculated in two steps. First, each component of the source term was approximated by superposition of scalar plane wave functions with different directions of propagation and frequencies. From these expansions, a particular solution for the Cauchy-Navier PDE was derived, at no extra computational cost, in the form of a linear combination of elastic P- and S-waves. In the second step, the homogeneous part of the solution was approximated via the classical MFS.

The proposed method was applied to two examples of the BVP, posed in a multiply-connected 2D domain. In the first case, where the exact solution of the BVP was known, accurate numerical results were obtained even with a relatively small number of test frequencies, unitary directions and collocation and source points. The results were improved by increasing the parameters of the method and this improvement was limited only by the maximum available machine precision.

In the second example, non-related body force and Dirichlet boundary data were considered. The quality of the approximate solution was analysed in terms of the domain collocation error of the body force approximation and the boundary error of the homogeneous part of the solution. Here, although accurate numerical results were also obtained, the increase of the precision was limited due to the singularity of the solution induced by the geometric singularities of the domain. In particular, the analytic basis functions of the MFS are insufficient for accurately fitting the solution in the neighborhood of the corners of the domain.

REFERENCES

[1] W. C. H. McLean, Strongly Elliptic Systems and Boundary Integral Equations. Cambridge University Press, Jun. 2010.

[2] V. D. Kupradze and M. A. Aleksidze, "The method of fundamental equa-tions for an approximate solution of certain boundary value problems," Comput Math Math Phys, vol. 4, pp. 82–126, 1964.

[3] R. Mathon and R. L. Johnson, "The approximate solution of elliptic boundary-value problems by fundamental solutions," SIAM J Numer Anal, vol. 14, pp. 638–650, 1977.

[4] A. H. D. Cheng and Y. Hong, "An overview of the method of fundamental solutions—Solvability, uniqueness, convergence, and stability," Engineering Analysis with Boundary Elements, vol. 120, pp. 118–152, nov 2020.

[5] G. Fairweather and A. Karageorghis, "The method of fundamental solutions for elliptic boundary value problems," Adv Comput Math, vol. 9, pp. 69–95, 1998.

[6] G. Fairweather, A. Karageorghis, and P. A. Martin, "The method of fun-damental solutions for scattering and radiation problems," Engineering Analysis with Boundary Elements, vol. 27, no. 7, pp. 759–769, jul 2003.

[7] A. Karageorghis, D. Lesnic, and L. Marin, "A survey of applications of the MFS to inverse problems," Inverse Problems in Science and Engineering, vol. 19, no. 3, pp. 309–336, apr 2011.

[8] C. Alves, A. Karageorghis, V. Leitao, and S. Valtchev, Eds., Advances in Trefftz Methods and Their Applications, ser. SEMA SIMAI Springer Series 23. Springer International Publishing, 2020.

[9] C. J. S. Alves, N. F. M. Martins, and S. S. Valtchev, "Extending the method of fundamental solutions to non-homogeneous elastic wave problems," Applied Numerical Mathematics, vol. 115, pp. 299–313, may 2017.

[10] P. W. Partridge, C. A. Brebbia, and L. C. Wrobel, The Dual Reciprocity Boundary Element Methods. Computational Mechanics Publications, Southampton, UK, 1992.

[11] G. C. de Medeiros, P. W. Partridge, and J. O. Brandao, "The method of fundamental solutions with dual reciprocity for some problems in elasticity," Engineering Analysis with Boundary Elements, vol. 28, no. 5, pp. 453–461, may 2004.

[12] C. C. Tsai, "The method of fundamental solutions with dual reciprocity for three-dimensional thermoelasticity under arbitrary body forces," Engineering Computations, vol. 26, no. 3, pp. 229–244, apr 2009.

[13] M. Khoshroo, M. Hematiyan, and Y. Daneshbod, "Two-dimensional elastodynamic and free vibration analysis by the method of fundamental solutions," Engineering Analysis with Boundary Elements, vol. 117, pp. 188–201, aug 2020.

[14] M. A. Golberg and C. S. Chen, "The method of fundamental solutions for potential, Helmholtz and diffusion problems," in Boundary Integral Methods: Numerical and Mathematical Aspects, M. A. Golberg, Ed., 1999, pp. 105–176.

[15] N. Piskunov, Differential and integral calculus. Moscow: Mir Publishers, 1969.

[16] R. Kress, Linear Integral Equations. Springer New York, 2014.

[17] V. D. Kupradze, Potential Methods in the Theory of Elasticity. Jerusalem: Israel Program for Scientific Translations, 1965.

[18] P. C. Hansen, Rank-Deficient and Discrete Ill-Posed Problems. SIAM, 1998.

[19] C. J. S. Alves and S. S. Valtchev, "Numerical comparison of two meshfree methods for acoustic wave scattering," Engineering Analysis with Boundary Elements, vol. 29, no. 4, pp. 371–382, apr 2005.

[20] F. Dou, L.-P. Zhang, Z.-C. Li, and C. S. Chen, "Source nodes on elliptic pseudo-boundaries in the method of fundamental solutions for Laplace's equation; selection of pseudo-boundaries," Journal of Computational and Applied Mathematics, vol. 377, p. 112861, oct 2020.

[21] C. S. Chen, A. Karageorghis, and Y. Li, "On choosing the location of the sources in the MFS," Numerical Algorithms, vol. 72, no. 1, pp. 107–130, aug 2015.

[22] C. J. Alves, "On the choice of source points in the method of fundamental solutions," Engineering Analysis with Boundary Elements, vol. 33, no. 12, pp. 1348–1361, dec 2009.

[23] P. R. S. Antunes and S. S. Valtchev, "A meshfree numerical method for acoustic wave propagation problems in planar domains with corners and cracks," Journal of Computational and Applied Mathematics, vol. 234, no. 9, pp. 2646–2662, sep 2010.